

Supplementary Information

Understanding the structure and mechanism of Na⁺ diffusion in NASICON solid-state electrolytes and the effect of Sc- and Al/Y- substitution

Ivana Pivarníková^{1,4}, Stefan Seidlmayer^{1,5}, Martin Finsterbusch², Gerald Dück², Niina Jalarvo³, Peter Müller-Buschbaum⁴, Ralph Gilles¹

¹ Heinz Maier-Leibnitz Zentrum (MLZ), Technical University of Munich, Lichtenbergstr.1,
85748, Garching, Germany

² Forschungszentrum Jülich GmbH, Institute of Materials and Devices, Materials Synthesis
and Processing (IMD-2), Wilhelm-Johnen-Strasse, 52425 Jülich, Germany

³ Neutron Sciences Directorate, Oak Ridge National Laboratory, Oak Ridge, Tennessee
37861-6475, USA

⁴ Technical University of Munich, TUM School of Natural Sciences, Department of Physics,
Chair for Functional Materials, James-Franck-Str. 1, 85748 Garching, Germany

^{5a} Department of Chemistry, Universität Bayreuth, Universitätsstrasse 30, 95447, Bayreuth,
Germany.

^{5b} Bavarian Center for Battery Technology (BayBatt), Universität Bayreuth, Weiherstrasse 26,
95448 Bayreuth, Germany

*Corresponding author contact:
Ivana Pivarníková (ivana.pivarnikova@frm2.tum.de)

Table S1: Ionic conductivity and D_{σ_bulk} values measured by EIS for NaZr, NaSc and NaAlY samples in the temperature range 173 – 423 K.

Na _{3.4} Zr ₂ Si _{2.4} P _{0.6} O ₁₂ (NaZr)				
Temperature [K]	σ_{bulk} [S cm ⁻¹]	σ_{gb} [S cm ⁻¹]	σ_{total} [S cm ⁻¹]	D_{σ_bulk} [cm ² s ⁻¹]
173	5.09 x 10 ⁻⁶	9.16 x 10 ⁻⁷	7.76 x 10 ⁻⁷	3.79 x 10 ⁻¹²
183	1.36 x 10 ⁻⁵	2.85 x 10 ⁻⁶	2.36 x 10 ⁻⁶	1.07 x 10 ⁻¹¹
203	7.25 x 10 ⁻⁵	1.92 x 10 ⁻⁵	1.52 x 10 ⁻⁵	6.35 x 10 ⁻¹¹
223	2.73 x 10 ⁻⁴	9.38 x 10 ⁻⁵	6.98 x 10 ⁻⁵	2.63 x 10 ⁻¹⁰
243	8.54 x 10 ⁻⁴	3.68 x 10 ⁻⁴	2.57 x 10 ⁻⁴	8.95 x 10 ⁻¹⁰
263	2.34 x 10 ⁻³	1.18 x 10 ⁻³	7.85 x 10 ⁻⁴	2.65 x 10 ⁻⁹
283	5.14 x 10 ⁻³	3.46 x 10 ⁻³	2.07 x 10 ⁻³	6.27 x 10 ⁻⁹
297	8.54 x 10⁻³	6.50 x 10⁻³	3.69 x 10⁻³	1.09 x 10⁻⁸
303	1.02 x 10 ⁻²	8.64 x 10 ⁻³	4.68 x 10 ⁻³	1.34 x 10 ⁻⁸
323	1.79 x 10 ⁻²	2.07 x 10 ⁻²	9.60 x 10 ⁻³	2.50 x 10 ⁻⁸
343	2.74 x 10 ⁻²	5.23 x 10 ⁻²	1.80 x 10 ⁻²	4.06 x 10 ⁻⁸
350	3.12 x 10 ⁻²	7.27 x 10 ⁻²	2.18 x 10 ⁻²	4.71 x 10 ⁻⁸
363	3.75 x 10 ⁻²	1.85 x 10 ⁻¹	3.12 x 10 ⁻²	5.87 x 10⁻⁸
383	-	-	5.08 x 10 ⁻²	
400	-	-	7.44 x 10 ⁻²	
403	-	-	7.83 x 10 ⁻²	
423	-	-	1.09 x 10 ⁻¹	
Na _{3.4} Sc _{0.4} Zr _{1.6} Si ₂ PO ₁₂ (NaSc)				
Temperature [K]	σ_{bulk} [S cm ⁻¹]	σ_{gb} [S cm ⁻¹]	σ_{total} [S cm ⁻¹]	D_{σ_bulk} [cm ² s ⁻¹]
173	1.27 x 10 ⁻⁶	6.65 x 10 ⁻⁷	4.36 x 10 ⁻⁷	9.36 x 10 ⁻¹³
183	3.83 x 10 ⁻⁶	2.05 x 10 ⁻⁶	1.34 x 10 ⁻⁶	3.00 x 10 ⁻¹²
203	2.43 x 10 ⁻⁵	1.45 x 10 ⁻⁵	9.06 x 10 ⁻⁶	2.10 x 10 ⁻¹¹
223	1.09 x 10 ⁻⁴	7.40 x 10 ⁻⁵	4.41 x 10 ⁻⁵	1.04 x 10 ⁻¹⁰
243	4.00 x 10 ⁻⁴	2.92 x 10 ⁻⁴	1.69 x 10 ⁻⁴	4.16 x 10 ⁻¹⁰
263	1.15 x 10 ⁻³	1.02 x 10 ⁻³	5.40 x 10 ⁻⁴	1.29 x 10 ⁻⁹
283	2.85 x 10 ⁻³	3.10 x 10 ⁻³	1.48 x 10 ⁻³	3.45 x 10 ⁻⁹
297	4.92 x 10⁻³	6.19 x 10⁻³	2.74 x 10⁻³	6.24 x 10⁻⁹
303	6.10 x 10 ⁻³	8.13 x 10 ⁻³	3.48 x 10 ⁻³	7.90 x 10 ⁻⁹
323	1.21 x 10 ⁻²	1.92 x 10 ⁻²	7.40 x 10 ⁻³	1.66 x 10 ⁻⁸
343	2.23 x 10 ⁻²	4.08 x 10 ⁻²	1.44 x 10 ⁻²	3.27 x 10 ⁻⁸
350	2.69 x 10 ⁻²	5.10 x 10 ⁻²	1.76 x 10 ⁻²	4.02 x 10 ⁻⁸
363	3.58 x 10 ⁻²	8.13 x 10 ⁻²	2.49 x 10 ⁻²	5.55 x 10⁻⁸
383	5.95 x 10 ⁻²	1.10 x 10 ⁻¹	3.86 x 10 ⁻²	9.73 x 10 ⁻⁸
400	-	-	5.31 x 10 ⁻²	
403	-	-	5.59 x 10 ⁻²	
423	-	-	7.60 x 10 ⁻²	
Na _{3.4} Al _{0.2} Y _{0.2} Zr _{1.6} Si ₂ PO ₁₂ (NaAlY)				
Temperature [K]	σ_{bulk} [S cm ⁻¹]	σ_{gb} [S cm ⁻¹]	σ_{total} [S cm ⁻¹]	D_{σ_bulk} [cm ² s ⁻¹]
173	6.77 x 10 ⁻⁷	2.67 x 10 ⁻⁸	2.57 x 10 ⁻⁸	5.06 x 10 ⁻¹³
183	1.96 x 10 ⁻⁶	8.72 x 10 ⁻⁸	8.35 x 10 ⁻⁸	1.55 x 10 ⁻¹²
203	1.16 x 10 ⁻⁵	6.25 x 10 ⁻⁷	5.93 x 10 ⁻⁷	1.02 x 10 ⁻¹¹
223	5.16 x 10 ⁻⁵	3.23 x 10 ⁻⁶	3.04 x 10 ⁻⁶	4.97 x 10 ⁻¹¹
243	1.33 x 10 ⁻⁴	1.36 x 10 ⁻⁵	1.23 x 10 ⁻⁵	1.39 x 10 ⁻¹⁰
263	6.07 x 10 ⁻⁴	4.31 x 10 ⁻⁵	4.03 x 10 ⁻⁵	6.90 x 10 ⁻¹⁰
283	1.42 x 10 ⁻³	1.19 x 10 ⁻⁴	1.10 x 10 ⁻⁴	1.74 x 10 ⁻⁹
297	2.52 x 10⁻³	2.20 x 10⁻⁴	2.02 x 10⁻⁴	3.23 x 10⁻⁹
303	3.06 x 10 ⁻³	2.84 x 10 ⁻⁴	2.59 x 10 ⁻⁴	4.00 x 10 ⁻⁹
323	5.63 x 10 ⁻³	6.13 x 10 ⁻⁴	5.52 x 10 ⁻⁴	7.85 x 10 ⁻⁹
343	9.24 x 10 ⁻³	1.22 x 10 ⁻³	1.08 x 10 ⁻³	1.37 x 10 ⁻⁸
350	1.20 x 10 ⁻²	2.36 x 10 ⁻³	1.97 x 10 ⁻³	1.81 x 10 ⁻⁸
363	1.63 x 10 ⁻²	4.21 x 10 ⁻³	3.34 x 10 ⁻³	2.55 x 10⁻⁸
383	-	-	4.99 x 10 ⁻³	
400	-	-	5.35 x 10 ⁻³	
403	-	-	8.29 x 10 ⁻³	
423	-	-	7.60 x 10 ⁻²	

Table S2: Diffusion parameters for NaZr, NaSc and NaAlY samples: the jump length (L) and residence time (τ) obtained from the fitting of Ch-E model to the Q-dependent HWHM of two Lorentzian functions. Calculated self-diffusion coefficients (D) are also listed here.

Na _{3.4} Zr _{2.4} P _{0.6} O ₁₂ (NaZr)			
broad Lorentzian \approx faster diffusion process			
T [K]	τ [ps]	L [\AA]	D [$\times 10^{-6} \text{ cm}^2 \text{ s}^{-1}$]
298	7.24 ± 4.69	1.38 ± 0.58	4.38 ± 4.67
350	7.65 ± 6.00	1.44 ± 0.66	4.51 ± 5.42
400	10.06 ± 3.89	1.70 ± 0.41	4.79 ± 2.95
450	11.92 ± 1.81	2.07 ± 0.23	6.02 ± 1.64
490	12.35 ± 2.16	2.09 ± 0.27	5.88 ± 1.83
540	12.05 ± 1.18	2.38 ± 0.18	7.85 ± 1.44
590	9.41 ± 0.34	2.95 ± 0.12	15.41 ± 1.40
640	7.19 ± 0.30	3.15 ± 0.13	22.94 ± 2.15
narrow Lorentzian \approx slower diffusion process			
T [K]	τ [ps]	L [\AA]	D [$\times 10^{-6} \text{ cm}^2 \text{ s}^{-1}$]
400	157 ± 47	1.81 ± 0.36	0.35 ± 2.27
450	215 ± 13	3.18 ± 0.20	0.78 ± 1.32
490	159 ± 15	3.38 ± 0.34	1.20 ± 1.79
540	111 ± 9	3.31 ± 0.28	1.65 ± 1.29
590	65 ± 6	3.00 ± 0.22	2.30 ± 1.10
640	48 ± 6	2.99 ± 0.30	3.10 ± 1.72
Na _{3.4} Sc _{0.4} Zr _{1.6} Si ₂ PO ₁₂ (NaSc)			
broad Lorentzian \approx faster diffusion process			
T [K]	τ [ps]	L [\AA]	D [$\times 10^{-6} \text{ cm}^2 \text{ s}^{-1}$]
298	9.33 ± 1.31	2.09 ± 0.48	7.83 ± 3.73
350	9.27 ± 0.90	2.18 ± 0.28	8.56 ± 2.31
400	10.46 ± 0.38	2.75 ± 0.14	12.04 ± 1.32
narrow Lorentzian \approx slower diffusion process			
T [K]	τ [ps]	L [\AA]	D [$\times 10^{-6} \text{ cm}^2 \text{ s}^{-1}$]
298	171 ± 28	2.64 ± 0.46	0.68 ± 0.26
350	167 ± 26	2.51 ± 0.39	0.62 ± 0.22
400	166 ± 26	2.43 ± 0.35	0.59 ± 0.20
Na _{3.4} Al _{0.2} Y _{0.2} Zr _{1.6} Si ₂ PO ₁₂ (NaAlY)			
broad Lorentzian \approx faster diffusion process			
T [K]	τ [ps]	L [\AA]	D [$\times 10^{-6} \text{ cm}^2 \text{ s}^{-1}$]
298	10.15 ± 1.05	5.64 ± 0.88	52.14 ± 17.15
400	13.30 ± 1.76	2.48 ± 0.30	7.68 ± 2.14
narrow Lorentzian \approx slower diffusion process			
T [K]	τ [ps]	L [\AA]	D [$\times 10^{-6} \text{ cm}^2 \text{ s}^{-1}$]
298	222 ± 37	2.54 ± 0.55	0.48 ± 0.22
400	210 ± 33	2.47 ± 0.36	0.49 ± 0.16

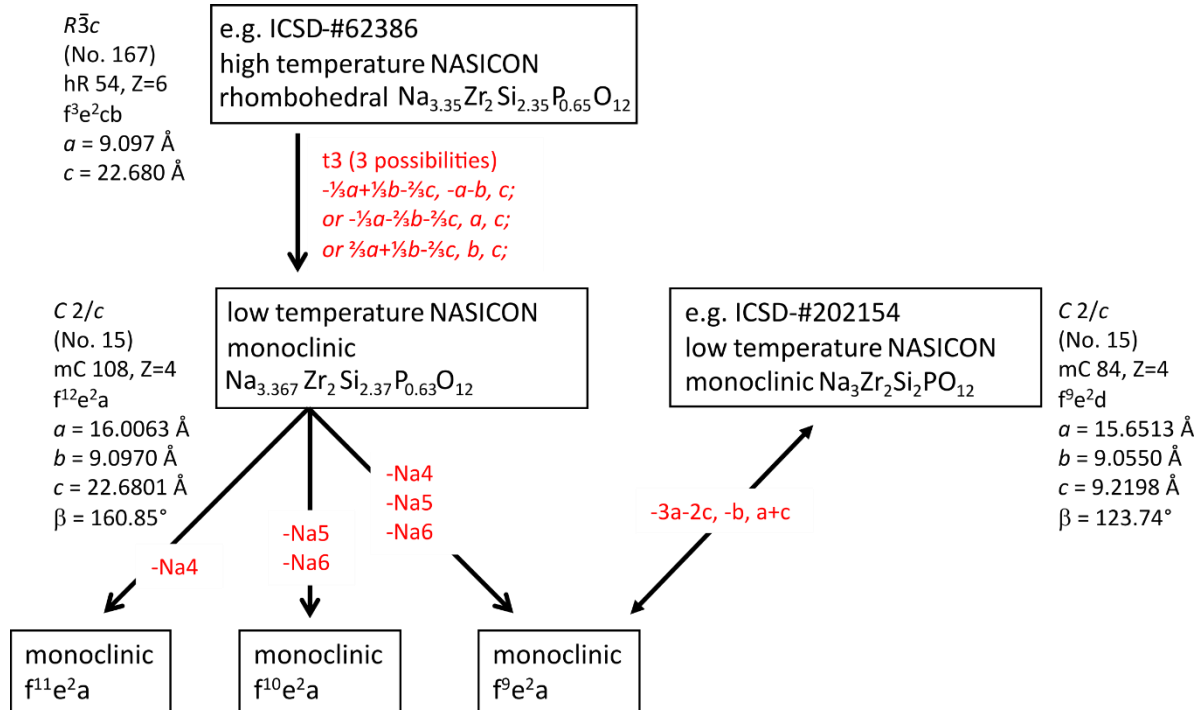


Figure S1: Group-subgroup relationship for the $R\bar{3}c \rightarrow C2/c$ phase transition and the relationship between the route to obtain different monoclinic structure models for the XRD Rietveld refinement. The starting point is the rhombohedral $R\bar{3}c$ f³e²cb model ICSD-#62386 by Boilot et al.¹ The connection between our f⁹e²a NASICON structure model and the usually published monoclinic NASICON structure model f⁹e²d is also shown (e.g. ICSD-#202154).²

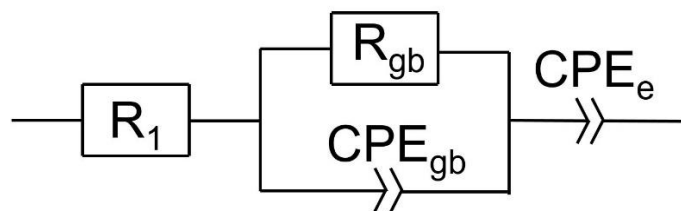


Figure S2: Nyquist Plots of EIS data were fitted using this equivalent circuit. With the resistance R and the constant phase element CPE, depending on the number of semi-circles that are visible at the investigated temperature. At low temperatures, the first semi-circle representing the bulk resistance becomes more pronounced, so the EC-model gets another CPE in parallel to R_1 .

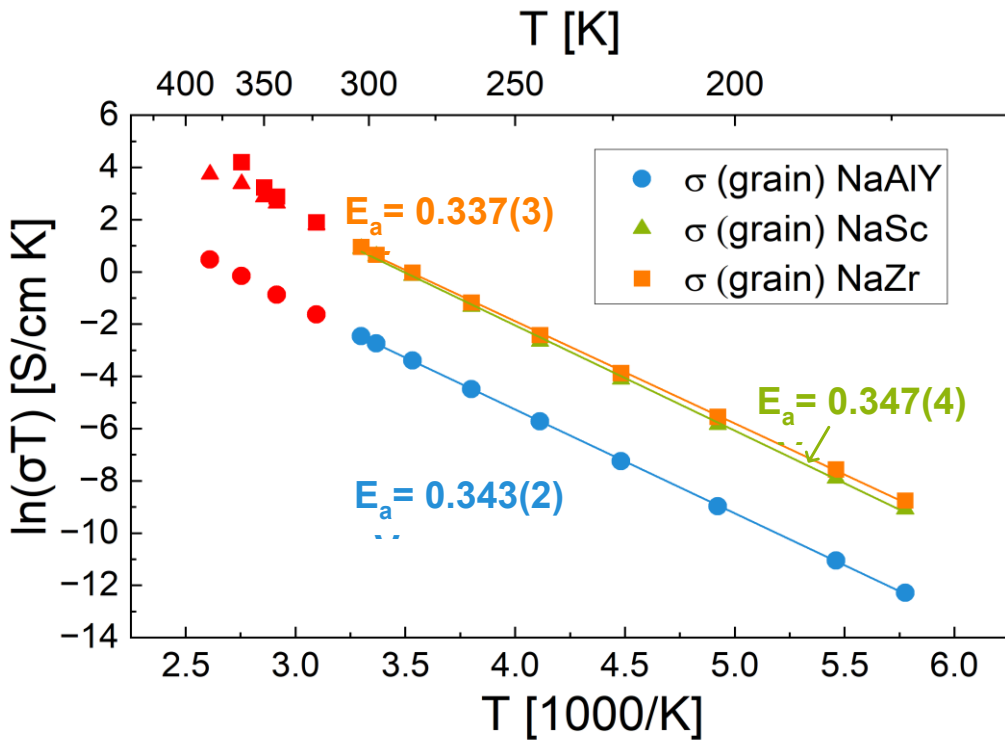


Figure S3: Arrhenius plot ($\ln(\sigma T)$ vs. $1/T$) of grain boundary conductivity (σ_{gb}) of $\text{Na}_{3.4}\text{Zr}_{2.4}\text{P}_{0.6}\text{O}_{12}$ (NaZr), $\text{Na}_{3.4}\text{Sc}_{0.4}\text{Zr}_{1.6}\text{Si}_2\text{PO}_{12}$ (NaSc) and $\text{Na}_{3.4}\text{Al}_{0.2}\text{Y}_{0.2}\text{Zr}_{1.6}\text{Si}_2\text{PO}_{12}$ (NaAlY) samples in the temperature range of 173 K to 423 K and the corresponding activation energies. Red data points are derived from less reliable fit parameters of impedance measurements. They were not considered to determine activation energies. PUT EV in

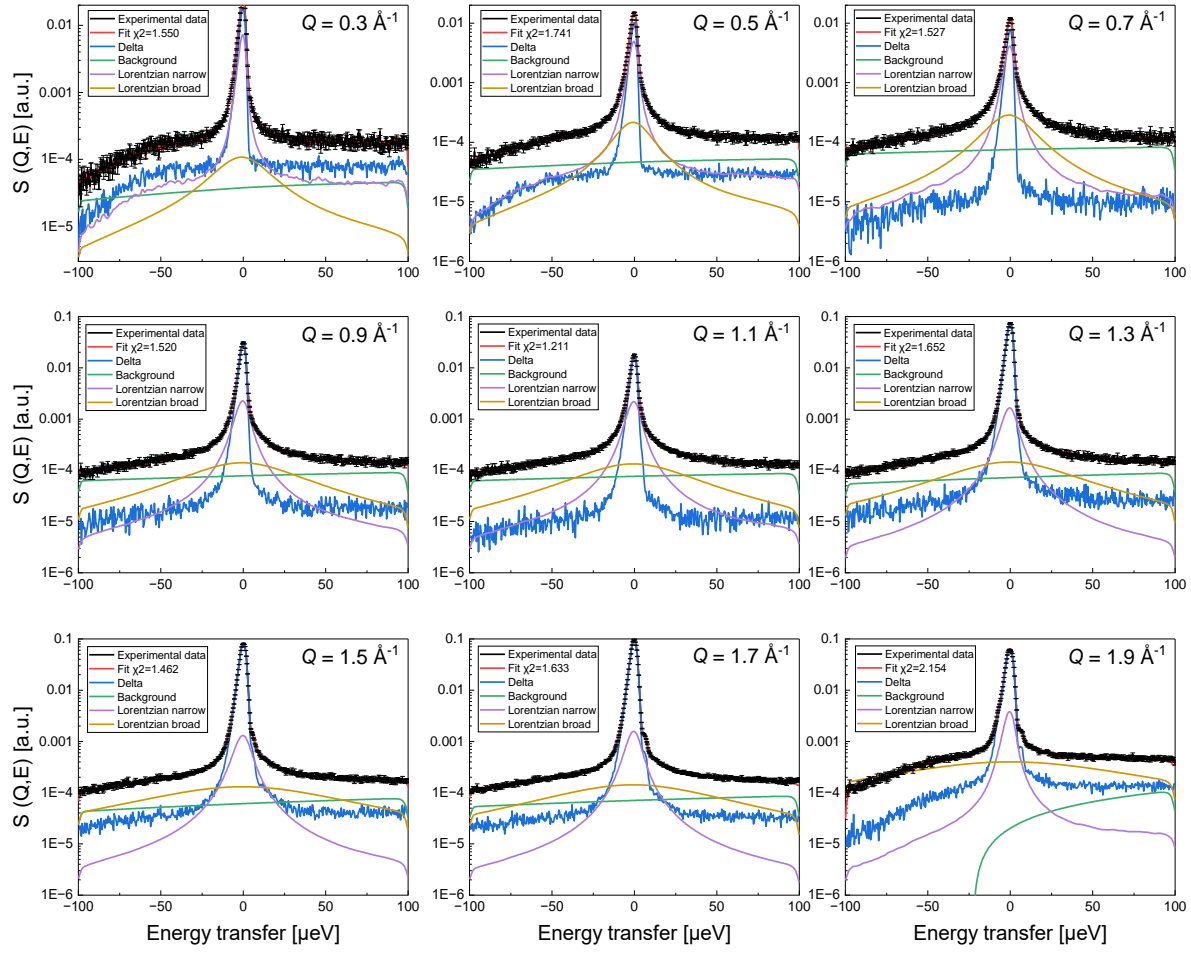


Figure S4: Selected QENS spectra for $\text{Na}_{3.4}\text{Zr}_2\text{Si}_{2.4}\text{P}_{0.6}\text{O}_{12}$ (NaZr): Dynamic structure factor $S(Q, E)$ as a function of energy transfer for all Q values in the range of $0.3 - 1.9 \text{ \AA}^{-1}$ at a temperature of 450 K. The black line represents the experimental data and the red line is the total fit of eq. (1) with corresponding χ^2 values. The background fit at the highest measured $Q = 1.9 \text{ \AA}^{-1}$ appears inaccurate on the logarithmic scale due to the highly asymmetric nature of the spectra, which complicates effective background modeling in this case.

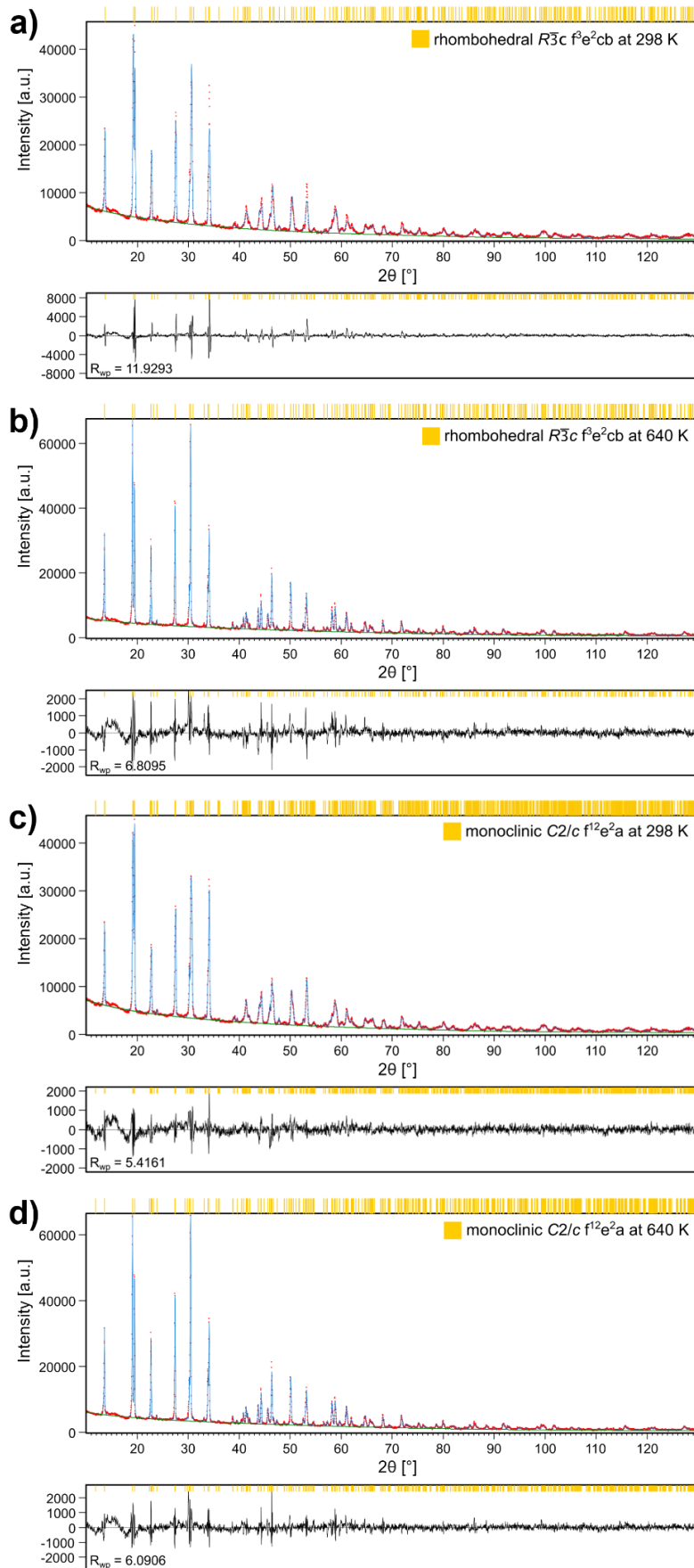


Figure S5: Selected full XRD patterns: Rietveld refinement of $\text{Na}_{3.4}\text{Zr}_2\text{Si}_{2.4}\text{P}_{0.6}\text{O}_{12}$ (NaZr): rhombohedral $R\bar{3}c$ f^3e^2cb at (a) 298 and (b) 640 K; monoclinic $C2/c$ $f^{12}e^2a$ at (c) 298 K (d) 640 K.

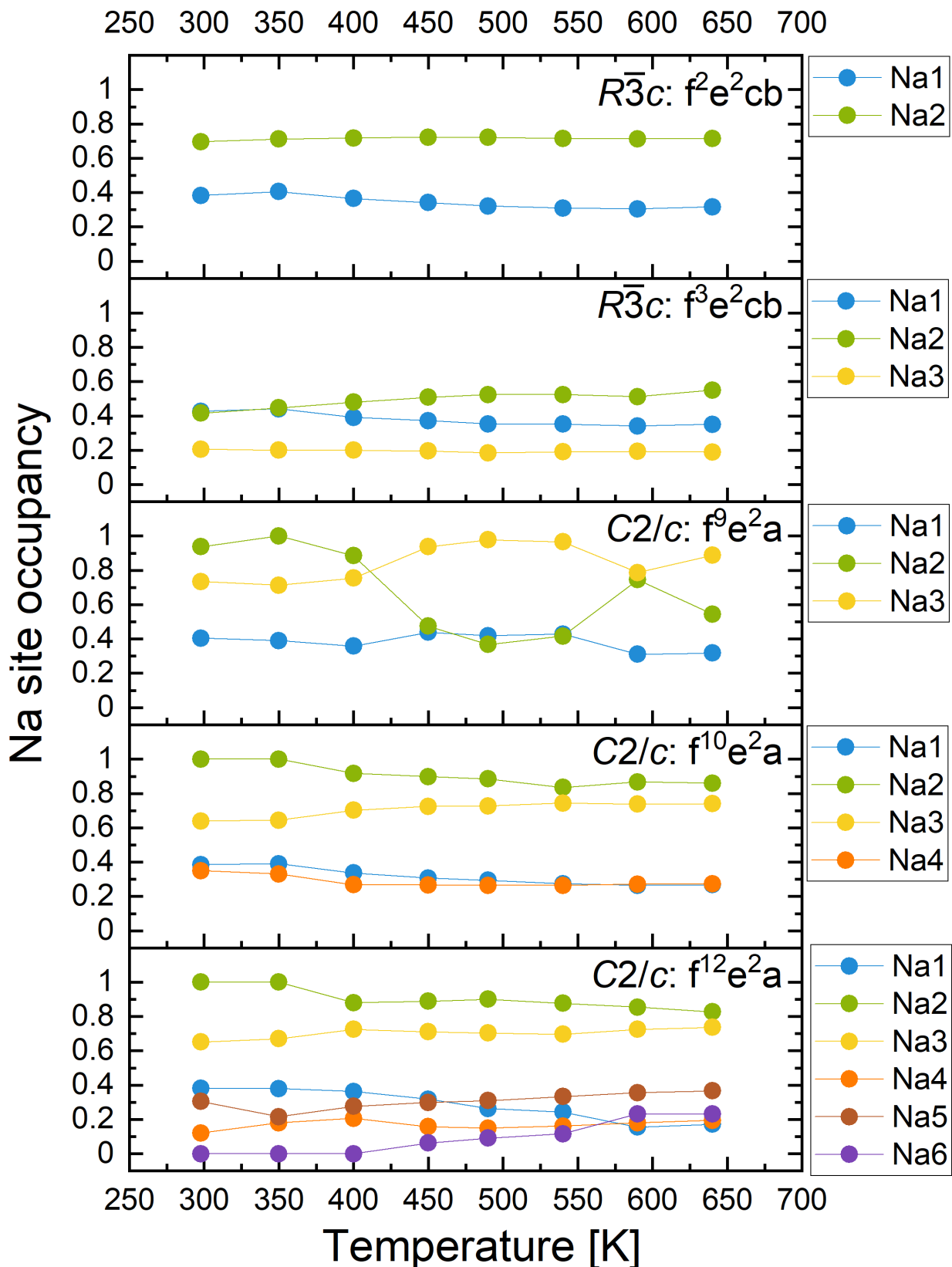


Figure S6: $\text{Na}_{3.4}\text{Zr}_2\text{Si}_{2.4}\text{P}_{0.6}\text{O}_{12}$ (NaZr): Na site occupancy for 5 different structural models and 6 different Na positions (Na1 6b, Na2 18e, and Na3, Na4, Na5, Na6 all 36f / 8f for monoclinic splitting). Solid lines are a guide to the eye.

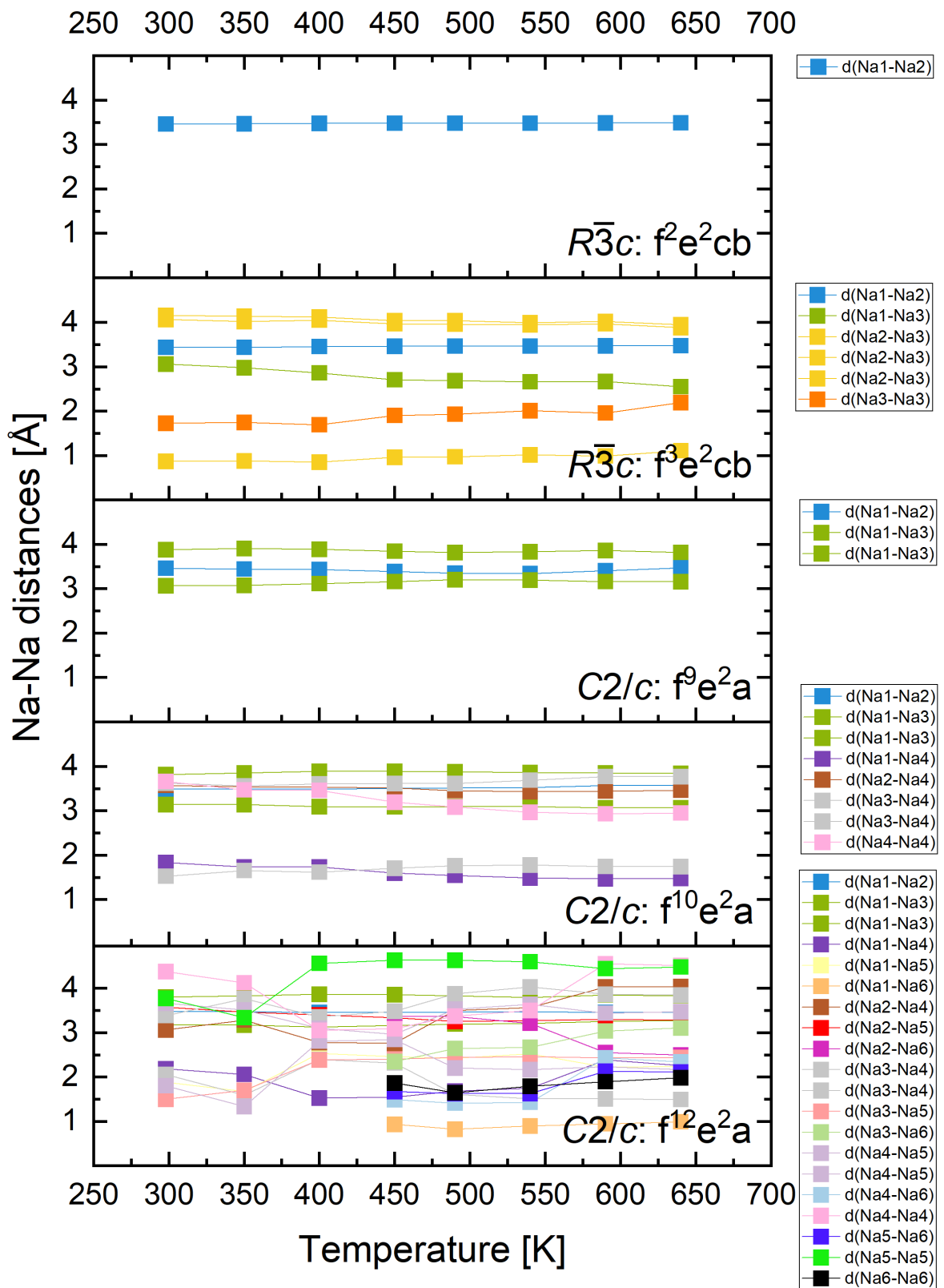


Figure S7: $\text{Na}_{3.4}\text{Zr}_2\text{Si}_{2.4}\text{P}_{0.6}\text{O}_{12}$ (NaZr): All refined Na-Na distances from XRD measurements and refinements for 5 different structural models and 6 different Na positions (Na1 6 b , Na2 18 e , and Na3, Na4, Na5, Na6 all 36 f / 8 f for monoclinic splitting). Solid lines are a guide to the eye.

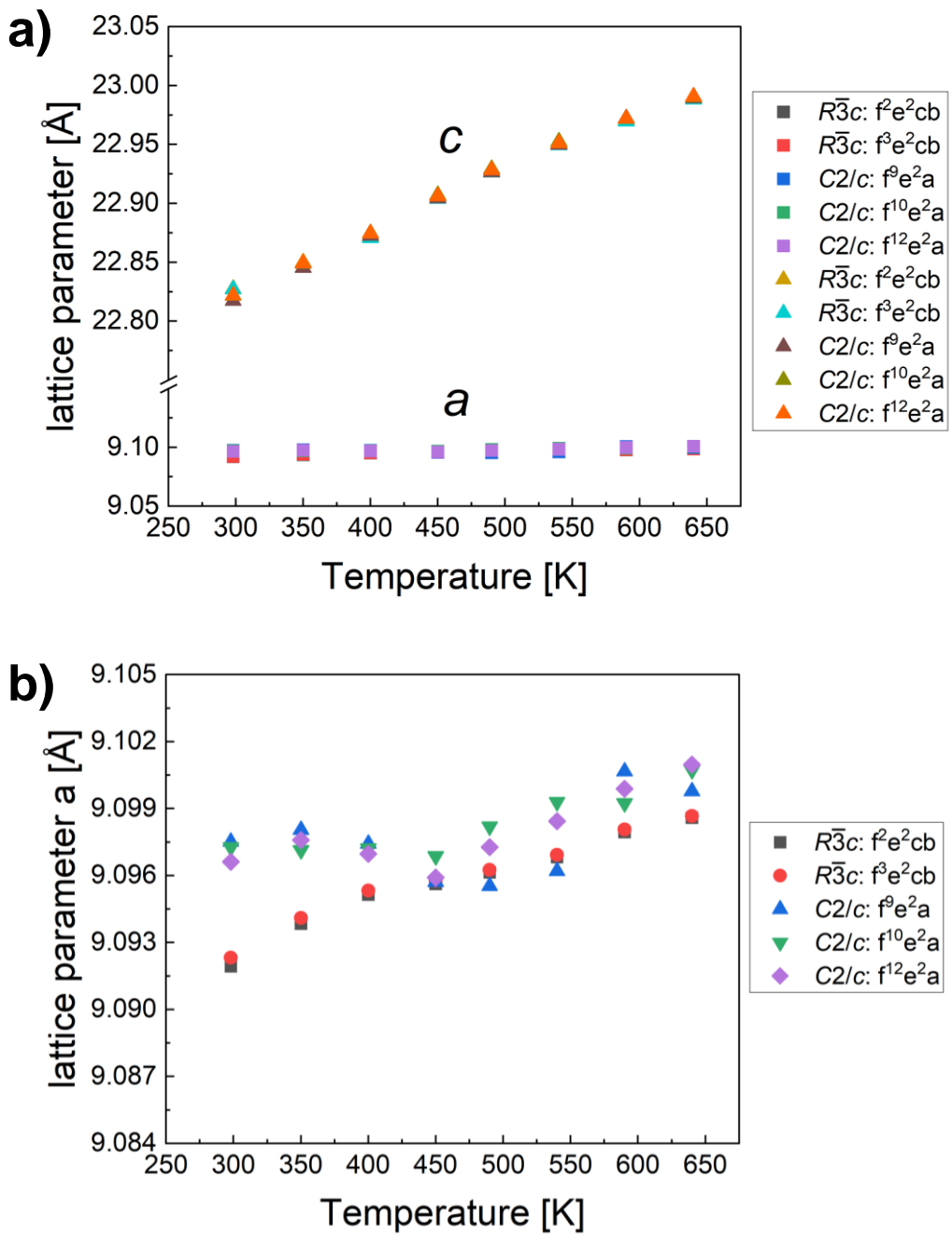


Figure S8: $\text{Na}_{3.4}\text{Zr}_2\text{Si}_{2.4}\text{P}_{0.6}\text{O}_{12}$ (NaZr): (a) Lattice parameters a (squares) and c (triangles) from XRD measurements for all refined structures and temperatures. For $\text{C}2/\text{c} f^{12}e^2a$, the thermal expansion coefficients (TEC) were calculated using linear fits. TEC for lattice parameter a is equal to $(1.289 \pm 0.383) \times 10^{-6} \text{ K}^{-1}$ and TEC for lattice parameter c is equal to $(2.226 \pm 0.007) \times 10^{-5} \text{ K}^{-1}$. The expansion in the c direction is more pronounced. They are in the same order of magnitude as previously reported values on NASICON.³ (b) close-up of the lattice parameter a : there are strong differences between the rhombohedral and monoclinic fits. The change in the temperature range of 400-450 K is consistent with the phase transition temperature.

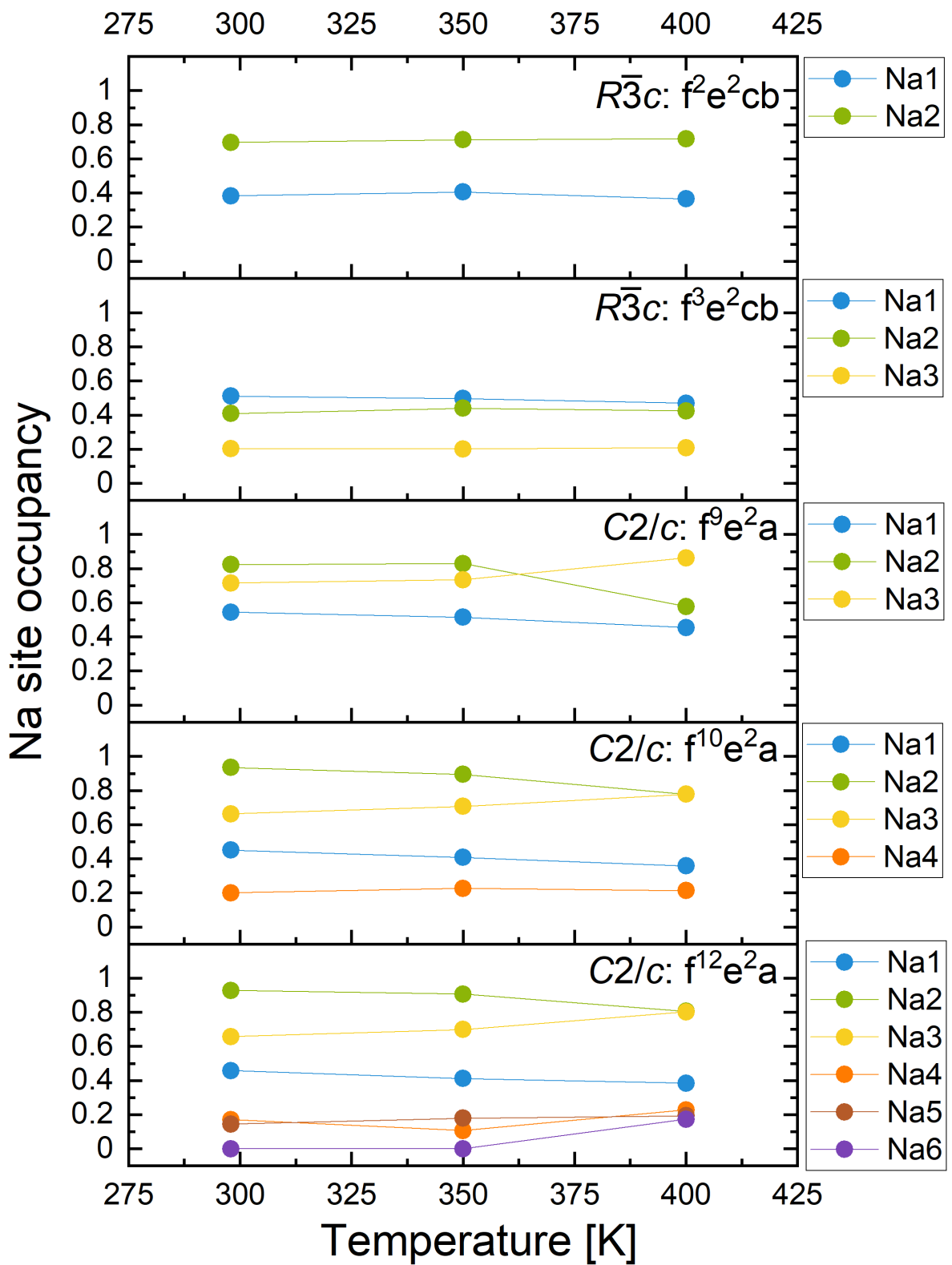


Figure S9: $\text{Na}_{3.4}\text{Sc}_{0.4}\text{Zr}_{1.6}\text{Si}_2\text{PO}_{12}$ (NaSc): Na site occupancy for 5 different structural models and 6 different Na positions (Na1 6b, Na2 18e, and Na3, Na4, Na5, Na6 all 36f / 8f for monoclinic splitting). Solid lines are a guide to the eye.

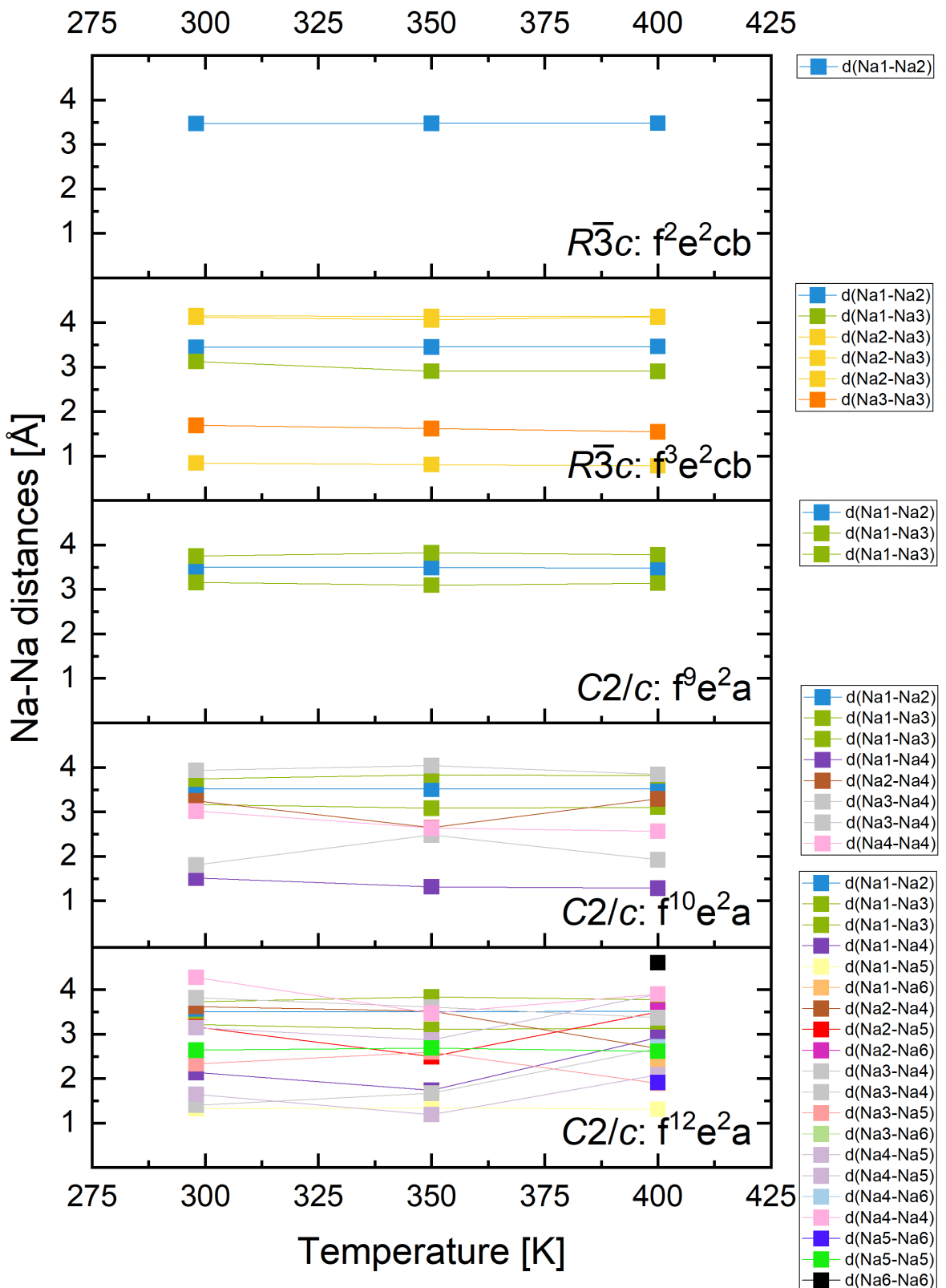


Figure S10: $\text{Na}_{3.4}\text{Sc}_{0.4}\text{Zr}_{1.6}\text{Si}_2\text{PO}_{12}$ (NaSc): All refined Na-Na distances from XRD measurements for 5 structural models and 6 different Na positions (Na1 6*b*, Na2 18*e*, and Na3, Na4, Na5, Na6 all 36*f* / 8*f* for monoclinic splitting). Solid lines are a guide to the eye.

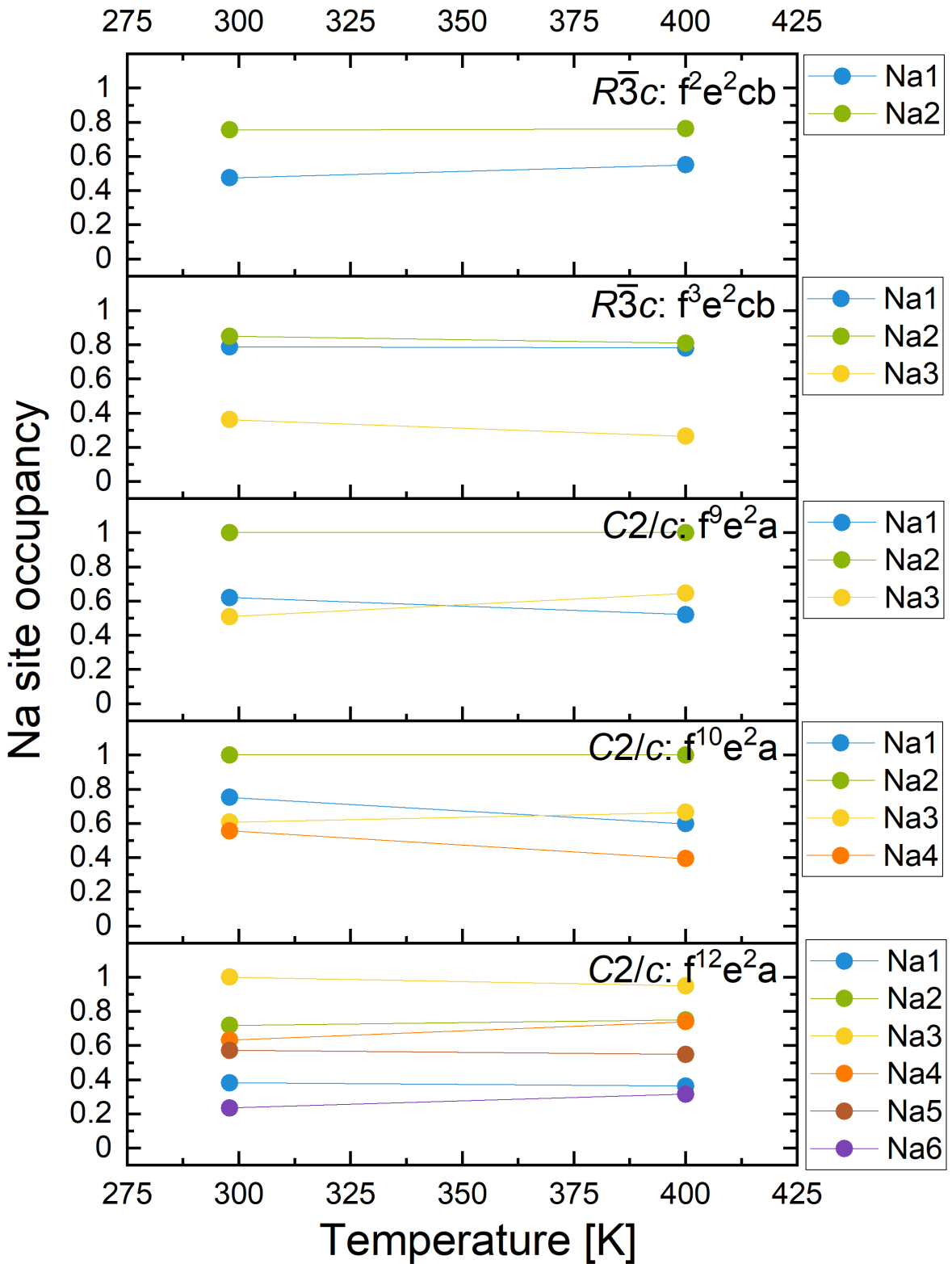


Figure S11: $\text{Na}_{3.4}\text{Al}_{0.2}\text{Y}_{0.2}\text{Zr}_{1.6}\text{Si}_2\text{PO}_{12}$ (NaAlY): Na site occupancy for 5 different structural models and 6 different Na positions (Na1 6 b , Na2 18 e , and Na3, Na4, Na5, Na6 all 36 f /8 f for monoclinic splitting). Solid lines are a guide to the eye.

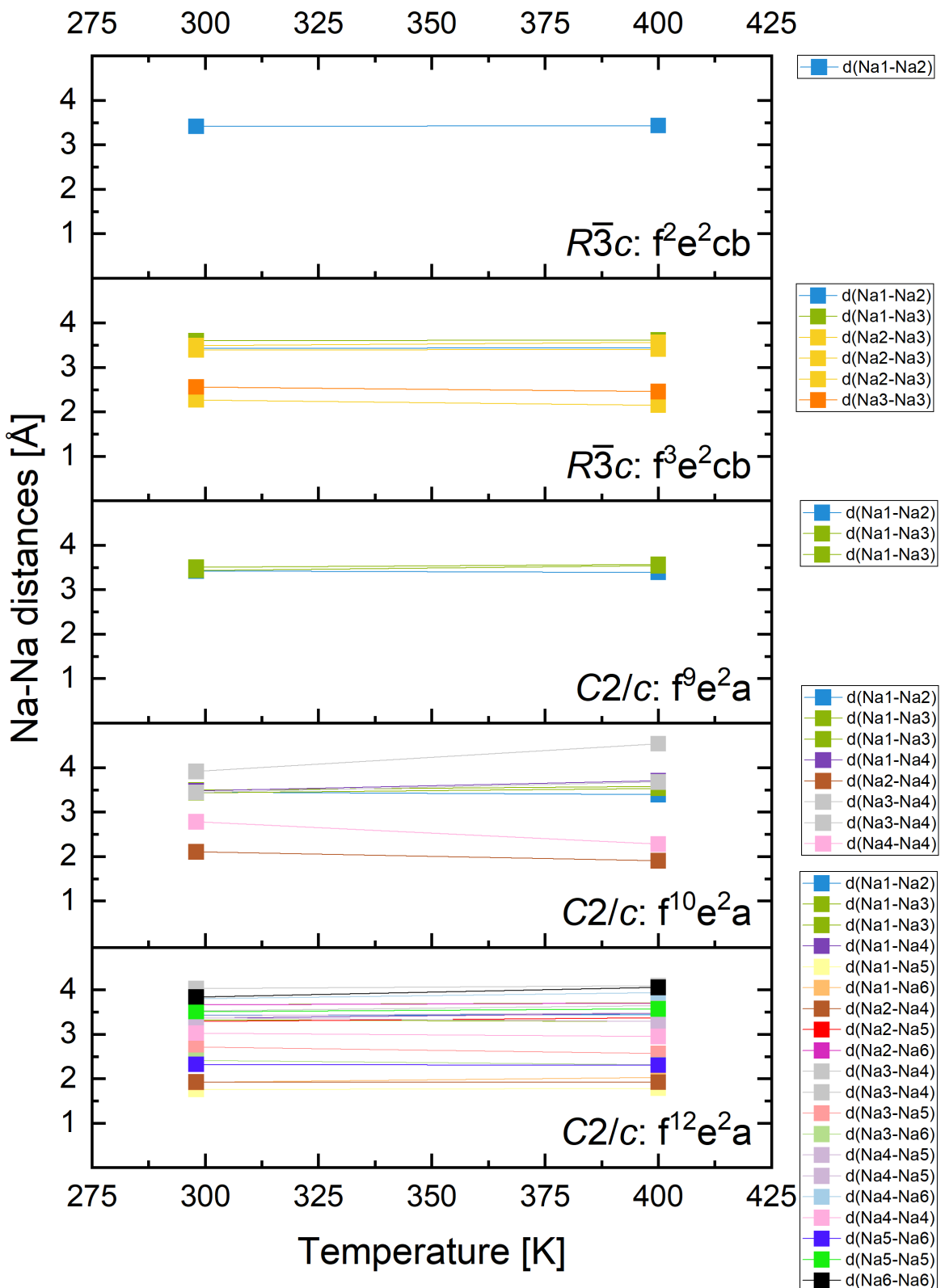


Figure S12: $\text{Na}_{3.4}\text{Al}_{0.2}\text{Y}_{0.2}\text{Zr}_{1.6}\text{Si}_2\text{PO}_{12}$ (NaAlY): All refined Na-Na distances from XRD measurements for 5 different structural models and 6 different Na positions (Na1 6*b*, Na2 18*e*, and Na3, Na4, Na5, Na6 all 36*f* / 8*f* for monoclinic splitting). Solid lines are a guide to the eye.

References

1. J.-P. Boilot, G. Collin and P. Colomban, *Journal of Solid State Chemistry*, 1988, **73**, 160-171.
2. W. H. Baur, J. R. Dygas, D. H. Whitmore and J. Faber, *Solid State Ionics*, 1986, **18-19**, 935-943.
3. Q. Ma, C.-L. Tsai, X.-K. Wei, M. Heggen, F. Tietz and J. T. Irvine, *Journal of Materials Chemistry A*, 2019, **7**, 7766-7776.